JACS
ARTICLES

Reversible C−C Coupling in a Uranium Biheterocyclic Complex

Marisa J. Monreal and Paula L. Diaconescu*

Department of Chemistry and Biochemistry, University of California, Los Angeles, California 90095

Received December 30, 2009; E-mail: pld@chem.ucla.edu

Abstract: The C−C coupling of two molecules of 1-methylbenzimidazole was effected by a neutral uranium dibenzyl complex supported by a ferrocene 1,1′-diamide ligand. The transformation involves the C−H activation of two heterocycles and the coupling of one η^2-N,C-imidazolyl fragment with a coordinated 1-methylbenzimidazole ligand. The solid-state structure of this product was studied by both single-crystal and powder X-ray diffraction methods and confirms the formation of the biheterocyclic moiety. In solution, the C−C coupling event was found to be reversible, as assessed by variable-temperature ^{1}H and ^{2}H NMR spectroscopy as well as DFT calculations and reactivity studies.
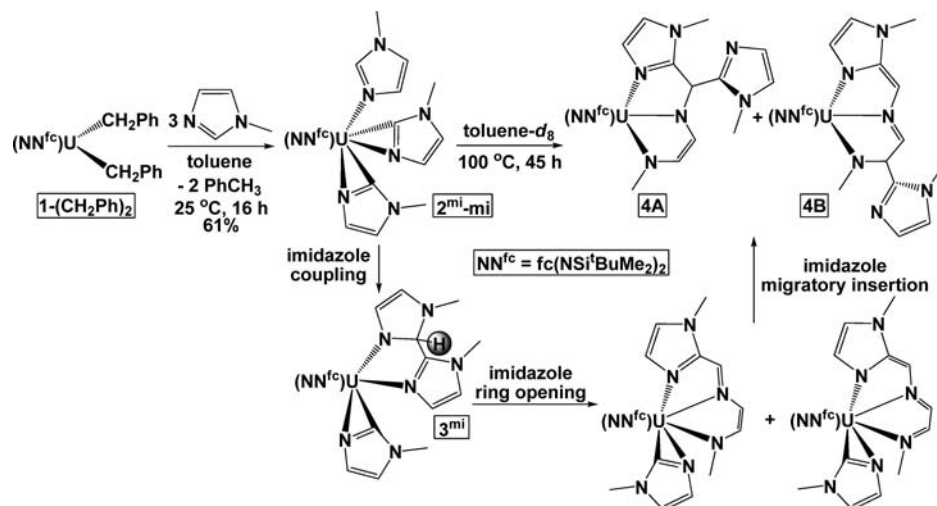
Introduction

The high Lewis acidity and large ionic radius of actinides often determine unique reactivity for their complexes.[1] Aromatic N-heterocycles represent interesting substrates both as synthetic targets[2] as well as hydrodenitrogenation models.[3] Actinide complexes engage in the functionalization as well as the cleavage of these molecules.[4] For example, cyclopentadienyl alkyl complexes of thorium have been shown to effect the ring-opening of pyridine N-oxides[5] after an initial C−H activation reaction.[6] It has also been reported that actinide complexes are more reactive than analogous group 4 complexes toward N-heterocycles, as shown by the fact that C−H activation occurs with neutral dialkyl complexes as opposed to the alkyl cationic complexes necessary for group 4.[7−9] The involvement of f electrons in covalent bonding can also be influential.[10−20] The combination of all these properties of uranium can lead to unexpected reactivity behaviors for its organometallic complexes.[21−28]

We have been investigating the reactivity of group 3[29−32] and uranium alkyl[33] complexes supported by a 1,1′-ferrocenylene-diamide ligand[34−36] toward aromatic N-heterocycles.[4,21,30,31,37−39] Uranium adds a new level of complexity since its ferrocene-diamide complexes have two alkyl groups that can both engage in reactions with the same substrate.

(1) Fox, A. R.; Bart, S. C.; Meyer, K.; Cummins, C. C. *Nature* **2008**, *455*, 341.
(2) Nakamura, I.; Yamamoto, Y. *Chem. Rev.* **2004**, *104*, 2127.
(3) Sanchez-Delgado, R. A. *Organometallic modelling of the hydrodesulfurization and hydrodenitrogenation reactions*; Kluwer Academic Publishers: Dordrecht, The Netherlands, 2002.
(4) Diaconescu, P. L. *Curr. Org. Chem.* **2008**, *12*, 1388.
(5) Pool, J. A.; Scott, B. L.; Kiplinger, J. L. *Chem. Commun.* **2005**, 2591.
(6) Pool, J. A.; Scott, B. L.; Kiplinger, J. L. *J. Am. Chem. Soc.* **2005**, *127*, 1338.
(7) Jantunen, K. C.; Scott, B. L.; Kiplinger, J. L. *J. Alloys Compd.* **2007**, *444−445*, 363.
(8) Pool, J. A.; Scott, B. L.; Kiplinger, J. L. *J. Alloys Compd.* **2006**, *418*, 178.
(9) Kiplinger, J. L.; Scott, B. L.; Schelter, E. J.; Pool Davis Tournear, J. A. *J. Alloys Compd.* **2007**, *444−445*, 477.
(10) Castro-Rodriguez, I.; Nakai, H.; Zakharov, L. N.; Rheingold, A. L.; Meyer, K. *Science* **2004**, *305*, 1757.
(11) Evans, W. J.; Kozimor, S. A.; Ziller, J. W. *Science* **2005**, *309*, 1835.
(12) Hayton, T. W.; Boncella, J. M.; Scott, B. L.; Palmer, P. D.; Batista, E. R.; Hay, P. J. *Science* **2005**, *310*, 1941.
(13) Summerscales, O. T.; Cloke, F. G. N.; Hitchcock, P. B.; Green, J. C.; Hazari, N. *Science* **2006**, *311*, 829.
(14) Diaconescu, P. L.; Arnold, P. L.; Baker, T. A.; Mindiola, D. J.; Cummins, C. C. *J. Am. Chem. Soc.* **2000**, *122*, 6108.
(15) Diaconescu, P. L.; Cummins, C. C. *J. Am. Chem. Soc.* **2002**, *124*, 7660.
(16) Cantat, T.; Graves, C. R.; Jantunen, K. C.; Burns, C. J.; Scott, B. L.; Schelter, E. J.; Morris, D. E.; Hay, P. J.; Kiplinger, J. L. *J. Am. Chem. Soc.* **2008**, *130*, 17537.
(17) Evans, W. J. *J. Alloys Compd.* **2009**, *488*, 493.
(18) Kozimor, S. A.; Yang, P.; Batista, E. R.; Boland, K. S.; Burns, C. J.; Clark, D. L.; Conradson, S. D.; Martin, R. L.; Wilkerson, M. P.; Wolfsberg, L. E. *J. Am. Chem. Soc.* **2009**, *131*, 12125.
(19) Kozimor, S. A.; Yang, P.; Batista, E. R.; Boland, K. S.; Burns, C. J.; Christensen, C. N.; Clark, D. L.; Conradson, S. D.; Hay, P. J.; Lezama, J. S.; Martin, R. L.; Schwarz, D. E.; Wilkerson, M. P.; Wolfsberg, L. E. *Inorg. Chem.* **2008**, *47*, 5365.
(20) Fox, A. R.; Cummins, C. C. *J. Am. Chem. Soc.* **2009**, *131*, 5716.
(21) Monreal, M. J.; Khan, S.; Diaconescu, P. L. *Angew. Chem., Int. Ed.* **2009**, *48*, 8352.
(22) Cantat, T.; Scott, B. L.; Morris, D. E.; Kiplinger, J. L. *Inorg. Chem.* **2009**, *48*, 2114.
(23) Cantat, T.; Graves, C. R.; Scott, B. L.; Kiplinger, J. L. *Angew. Chem., Int. Ed.* **2009**, *48*, 3681.
(24) Evans, W. J.; Traina, C. A.; Ziller, J. W. *J. Am. Chem. Soc.* **2009**, *131*, 17473.
(25) Evans, W. J.; Montalvo, E.; Kozimor, S. A.; Miller, K. A. *J. Am. Chem. Soc.* **2008**, *130*, 12258.
(26) Evans, W. J.; Kozimor, S. A. *Coord. Chem. Rev.* **2006**, *250*, 911.
(27) Fortier, S.; Hayton, T. W. *Coord. Chem. Rev.* **2010**, *254*, 197.
(28) Schnaars, D. D.; Wu, G.; Hayton, T. W. *J. Am. Chem. Soc.* **2009**, *131*, 17532.
(29) Carver, C. T.; Monreal, M. J.; Diaconescu, P. L. *Organometallics* **2008**, *27*, 363.
(30) Carver, C. T.; Benitez, D.; Miller, K. L.; Williams, B. N.; Tkatchouk, E.; Goddard, W. A.; Diaconescu, P. L. *J. Am. Chem. Soc.* **2009**, *131*, 10269.
(31) Miller, K. L.; Williams, B. N.; Benitez, D.; Carver, C. T.; Ogilby, K. R.; Tkatchouk, E.; Goddard, W. A.; Diaconescu, P. L. *J. Am. Chem. Soc.* **2010**, *132*, 342.
(32) Jie, S.; Diaconescu, P. L. *Organometallics* **2010**, *29*, 1222.
(33) Monreal, M. J.; Diaconescu, P. L. *Organometallics* **2008**, *27*, 1702.

Recently, we reported a novel C−H activation reaction by $(NN^{fc})U(CH_2Ph)_2$, **1-(CH₂Ph)₂** (NN^{fc} = $fc(NSi^tBuMe_2)_2$, fc = 1,1′-ferrocenylene)[33] and showed that both benzyl ligands of **1-(CH₂Ph)₂** reacted with an sp^2 C−H bond of 1-methylimidazole (mi) to give **2^{mi}-mi** (Scheme 1).[21] We have also shown that, after the C−H activation events, an interesting cascade of functionalization reactions can be thermally induced. Specifically, upon heating, **2^{mi}-mi** undergoes C−C coupling to give **3^{mi}**, ring-opening, and migratory insertion of the imidazole ligands to lead, ultimately, to an isomeric mixture of **4A** and **4B** (Scheme 1). The products **4A** and **4B** feature three modified imidazole fragments; the cascade of reactions leading to them represents the first example of aromatic N-heterocycle cleavage by actinide complexes where no oxygen atoms[5] or redox processes[40] are involved.

During our studies, we attempted to mimic the reactions of 1-methylimidazole and **1-(CH₂Ph)₂** with 1-methylbenzimidazole in order to determine whether similar results would be obtained. A complex analogous to **3^{mi}**, **3^{mbi}**, was isolated and characterized by single-crystal X-ray crystallography, providing support for the mechanistic proposal presented in Scheme 1.[21] To our surprise, the solid-state structure of **3^{mbi}** did not agree with the solution structure as assessed by ¹H NMR spectroscopy; the number of peaks observed was too low when compared to that expected based on the asymmetry of the solid-state structure. Herein, we report that the C−C coupling event resulting in the formation of **3^{mbi}** is reversible. This unexpected equilibrium was characterized extensively by variable temperature ¹H and ²H NMR spectroscopy, X-ray powder diffraction, DFT calculations, and reactivity studies. Reversible bond formation has been invoked as the basis for developing switchable molecular systems and the C−C bond formation involving heterocycles has been recently identified as a fruitful area for exploration.[41−43] In general, such a system switches between two states in

response to an external stimulus; however, the results discussed herein show that the two states may coexist in solution for **3^{mbi}**.

Results and Discussion

Synthesis and Solid-State Characterization of Complexes. The reaction between **1-(CH₂Ph)₂** and three equivalents of 1-methylbenzimidazole led to large red-brown crystals of **3^{mbi}** from concentrated hexanes at −35 °C in 88% yield (eq 1). The initial interpretation of the ¹H NMR spectrum of **3^{mbi}** indicated a C_{2v}-symmetrical complex: peak integrations matched a compound with two C−H activated 1-methylbenzimidazole ligands. A similar situation was observed for the room-temperature ¹H NMR spectrum of **2^{mi}-mi**. However, the solid-state structure of **3^{mbi}** determined by X-ray crystallography illustrated a different result (Figure 1): instead of two simple ortho-metalation events, C−C coupling of two 1-methylbenzimidazole ligands and dearomatization of one of rings had also occurred. Interestingly, the solid-state structure of **2^{mi}-mi** (Figure 1) is different from that of **3^{mbi}** even though the two complexes were synthesized by analogous reactions. Although both crystal structures were reported in a previous communication,[21] representations and a discussion are included herein for ease of reference.

There are two previously reported examples similar to **3^{mbi}**: one is a proposed (but uncharacterized) intermediate in the
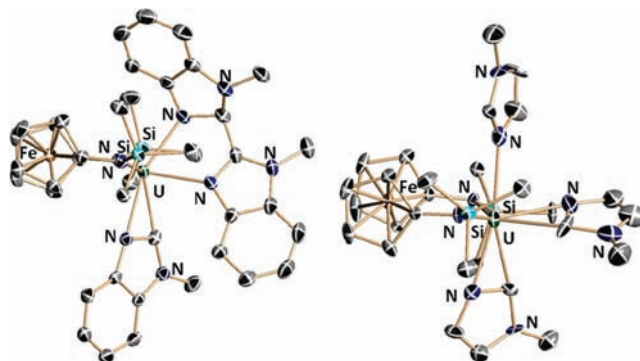
(34) Shafir, A.; Power, M. P.; Whitener, G. D.; Arnold, J. *Organometallics* **2000**, *19*, 3978.
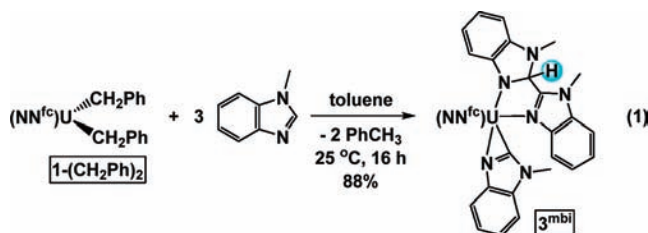(35) Shafir, A.; Arnold, J. *J. Am. Chem. Soc.* **2001**, *123*, 9212.
(36) Monreal, M. J.; Carver, C. T.; Diaconescu, P. L. *Inorg. Chem.* **2007**, *46*, 7226.
(37) Carver, C. T.; Diaconescu, P. L. *J. Alloys Compd.* **2009**, *488*, 518.
(38) Carver, C. T.; Diaconescu, P. L. *J. Am. Chem. Soc.* **2008**, *130*, 7558.
(39) Carver, C. T.; Williams, B. N.; Ogilby, K. R.; Diaconescu, P. L. *Organometallics* **2010**, *29*, 835.
(40) Arunachalampillai, A.; Crewdson, P.; Korobkov, I.; Gambarotta, S. *Organometallics* **2006**, *25*, 3856.

Figure 1. Thermal-ellipsoid (50% probability) representation of **3^{mbi}** (left) and **2^{mi}-mi** (right); H, solvent atoms, and ^tBu methyl groups were removed for clarity.

reaction between Cp*$_2$Y(η^2-N,C-pyridyl) and excess pyridine,[44] the other is the coupling of pyridines or imidazoles by group 3 alkyl complexes supported by a 1,1′-ferrocenylene-diamide ligand, from our group.[38,39] In a report specific to uranium, the synthesis of Cp$^\#_4$U$_6$O$_{13}$(bipy)$_2$ (Cp$^\#$ = 1,2,4-^{t}Bu$_3$C$_5$H$_2$; bipy = 2,2′-bipyridine) from Cp$^\#_2$UCl$_2$, KC$_8$, and pyridine-*N*-oxide, was explained by proposing that two pyridyl radicals combined to form 2,2′-bipyridine.[45] To our knowledge, no imidazole C−C coupling product has been previously isolated and characterized either for a uranium or a transition metal complex prior to our study.[21] A complicated reaction, in which an N-heterocyclic carbene was used as a precursor, led to a rhodium complex with a structure relatively similar to that of **3^{mbi}**, but a procedure for the synthesis of this complex was not included, likely because of the complex nature of the reaction from which it was separated.[46]

The comparison of metrical parameters for **3^{mbi}** and **2^{mi}-mi** is informative. The complex **3^{mbi}** features a short U−N$_{mbi}$ distance of 2.3891(39) Å, corresponding to the bond between uranium and the amide nitrogen of the dearomatized heterocycle, an intermediate U−N$_{mbi}$ distance of 2.4372(39) Å to the other nitrogen donor of the biheterocyclic fragment, and a long U−N$_{mbi}$ distance of 2.5136(41) Å to the η^2-N,C-imidazolyl ligand. Metrical parameters are also consistent with the dearomatization of one of the imidazole rings in **3^{mbi}**. For example, the N−C distances in the heteroaromatic ring of the biheterocyclic structure are 1.3323(59), 1.3984(61), 1.3609(60), and 1.3881(66) Å, while in the dearomatized ring they are 1.3870(64), 1.4593(62), 1.4137(67), and 1.4692(63) Å, with the two longest distances being to the sp^3-carbon atom. The NCN angle of 104.95(40)° and the NCC angles of 109.29(39) and 114.47(41)° around the sp^3-carbon atom also support the above structural assignment. The distances involving the η^2-N,C-imidazolyl ligands are similar in **3^{mbi}** (U−C$_U$, 2.4455(49) Å; N$_U$−C$_U$, 1.3464(57) Å; N−C$_U$, 1.3644(60) Å; N$_U$−C, 1.4003(58) Å; C−C, 1.3998(64) Å; N−C, 1.3925(60) Å) and **2^{mi}-mi** (U−C$_U$, 2.467(16) and 2.474(16) Å; N$_U$−C$_U$, 1.362(20) and 1.381(28) Å; N−C$_U$, 1.422(19) and 1.454(23) Å; N$_U$−C, 1.376(20) and 1.417(24) Å; C−C, 1.322(23) and 1.238(28) Å; N−C, 1.422(19) and 1.325(25) Å).

To ensure that the crystal chosen for the structure determination of **3^{mbi}** was not merely an isolated example, a crystal from a separate batch was also characterized by X-ray crystallography and found to have the same structure. The unit cell of
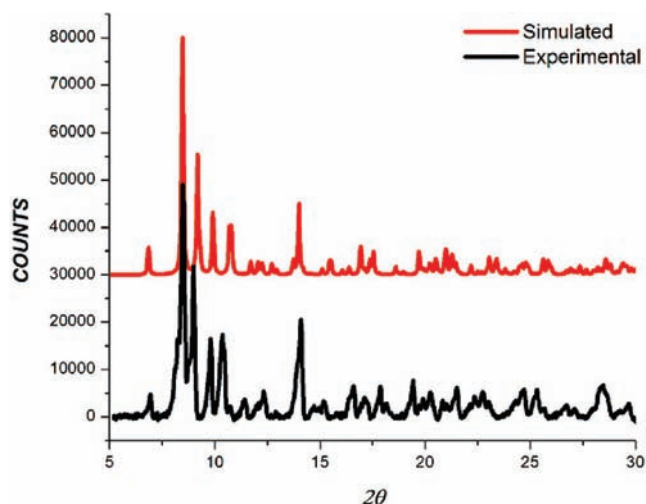
(41) Kitson, P. J.; Parenty, A. D. C.; Richmond, C. J.; Long, D.-L.; Cronin, L. *Chem. Commun.* **2009**, 4067.
(42) Weber, C.; Rustemeyer, F.; Dürr, H. *Adv. Mater.* **1998**, *10*, 1348.
(43) Rao, Y.-L.; Amarne, H.; Zhao, S.-B.; McCormick, T. M.; Martiæ, S.; Sun, Y.; Wang, R.-Y.; Wang, S. *J. Am. Chem. Soc.* **2008**, *130*, 12898.
(44) Deelman, B.-J.; Stevels, W. M.; Teuben, J. H.; Lakin, M. T.; Spek, A. L. *Organometallics* **1994**, *13*, 3881.
(45) Duval, P. B.; Burns, C. J.; Clark, D. L.; Morris, D. E.; Scott, B. L.; Thompson, J. D.; Werkema, E. L.; Jia, L.; Andersen, R. A. *Angew. Chem., Int. Ed.* **2001**, *40*, 3357.
(46) Mas-Marza, E.; Poyatos, M.; Sanau, M.; Peris, E. *Inorg. Chem.* **2004**, *43*, 2213.

Figure 2. Powder X-ray diffraction data for compound **3^{mbi}**. (Top) Simulated pattern derived from single-crystal X-ray diffraction data. (Bottom) Data collected from a microcrystalline sample.

Scheme 2. Proposed Solution Equilibrium for **2^{mi}-mi**
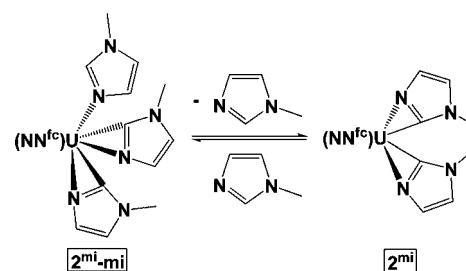
a crystal from a third batch was identical to the first two. Furthermore, a powder X-ray diffraction study was conducted on a microcrystalline sample of **3^{mbi}**. The resulting pattern from this experiment matched the simulated pattern derived from the single-crystal X-ray data (Figure 2), indicating that, in the solid state, the structure of compound **3^{mbi}** is consistent with the presence of two coupled imidazole rings.

Solution Structures. An investigation of the ^{1}H NMR spectra (C$_6$D$_6$, 25 °C) of **2^{mi}-mi** and **3^{mbi}** was undertaken to elucidate the observation of symmetrical species in solution. In the room-temperature ^{1}H NMR spectra of **2^{mi}-mi** or **3^{mbi}**, only one set of peaks was observed for the *t*-butyl or methyl groups of the ancillary ligand as well as for the two imidazole ligands. Small, broad peaks were apparent in the spectrum of **2^{mi}-mi** and were attributed to the labile 1-methylimidazole fragment. In order to support this assignment, an excess of 1-methylimidazole was added to **2^{mi}-mi**; the broad peaks proportionally increased in intensity and the ligand peaks shifted, consistent with the complex being involved in a coordination/dissociation equilibrium with 1-methylimidazole (Scheme 2 and Figure 3, left).

An analogous ^{1}H NMR spectrum (C$_6$D$_6$, 25 °C) was obtained for **3^{mbi}**: peak integrations of the sharp signals matched a compound with two ortho-metalated 1-methylbenzimidazole ligands. In addition to the sharp signals, very broad signals were also observed at ca. 10 − 25 ppm (Figure 3, right). It is proposed that the broad resonances correspond to a coordinated 1-methylbenzimidazole ligand, as in **2^{mbi}-mbi**, which engages in a fast exchange with free 1-methylbenzimidazole at room temperature, similar to what was observed for **2^{mi}-mi** (Scheme 2). To find support for this proposal, the reactions of **1-(CH$_2$Ph)$_2$** with
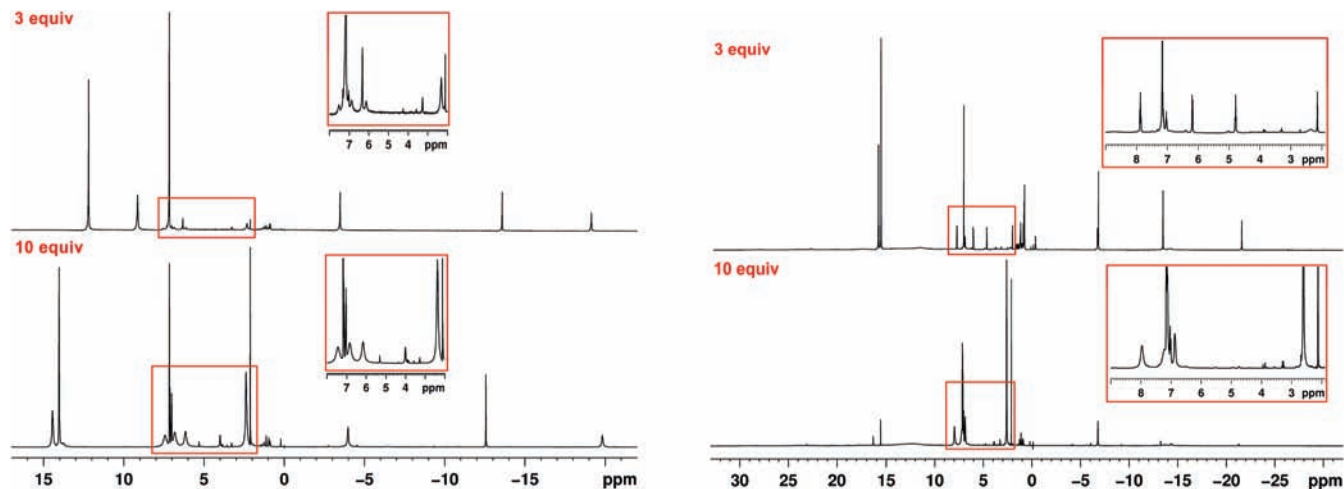
Figure 3. (*Left*) ^{1}H NMR spectra (25 °C, 500 MHz, C_6D_6) of the reaction between **1-(CH$_2$Ph)$_2$** and 1-methylimidazole (top, 3 equivalents; bottom, 10 equivalents) consistent with the equilibrium shown in Scheme 2. (*Right*) ^{1}H NMR spectra (25 °C, 500 MHz, C_6D_6) of the reaction between **1-(CH$_2$Ph)$_2$** and 1-methylbenzimidazole (top, 3 equiv; bottom, 10 equiv) consistent with the equilibria shown in Scheme 3.

Scheme 3. Proposed Solution Equilibria for **3^{mbi}**
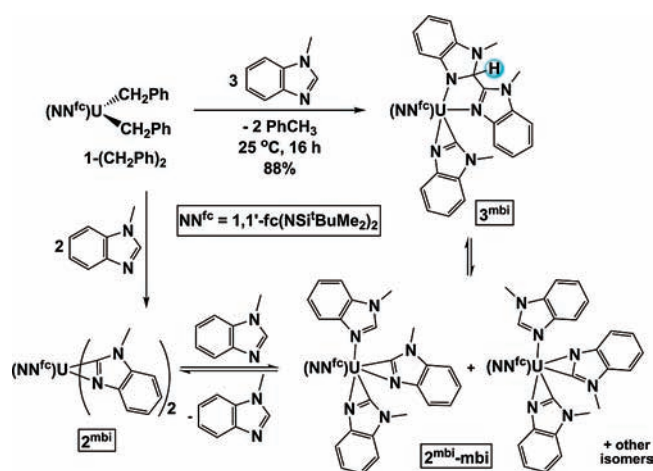
1-methylbenzimidazole with 3 and 10 equivalents were investigated by ^{1}H NMR spectroscopy (Figure 3, right).

In order to reconcile the solution and the solid-state structures, we propose that *a reversible C−C coupling event*, which transforms **3^{mbi}** into **2^{mbi}-mbi**, takes place (Scheme 3). This hypothesis was initially probed by variable-temperature (VT) ^{1}H NMR spectroscopy studies. When a solution of isolated crystals of **3^{mbi}** was cooled from room temperature to ca. −90 °C, several new peaks became visible in the ^{1}H NMR spectra (Figure 4, left). These new peaks are attributed to multiple unsymmetrical species. These species may be **3^{mbi}** (expected to have a larger number of peaks than the symmetrical **2^{mbi}**) and/or different isomers of **2^{mbi}-mbi** (Scheme 3, see the Supporting Information for other possible isomers), implying that the equilibria shown in Scheme 3 shift toward the mixture of **2^{mbi}-mbi** isomers and, possibly, **3^{mbi}**, as the temperature decreases. Because the cleavage of the C−C bond between the two coupled imidazole rings could give rise to different isomers of **2^{mbi}-mbi** (formation of the U−C bond may occur on the same time scale as rotation around different U−N bonds), more than one isomer of **2^{mbi}-mbi** may be present in solution. Therefore, **3^{mbi}** could exist in solution in equilibrium with isomers of **2^{mbi}-mbi**. Since all complexes involved are paramagnetic, it is not possible to distinguish between **3^{mbi}** and various **2^{mbi}-mbi**

isomers, a fact that complicates the definitive identification of all species present in solution.

Extended solution NMR spectroscopy studies provided further support for the reversibility of the C−C coupling event. Importantly, when **2^{mbi}** was generated in situ from the reaction between **1-(CH$_2$Ph)$_2$** and exactly two equivalents of 1-methylbenzimidazole and subjected to the same VT ^{1}H NMR analysis, no new peaks became visible upon cooling (Figure 4, right). This finding corroborates the hypothesis that with only two equivalents of 1-methylbenzimidazole present, **2^{mbi}** cannot undergo the proposed equilibrium, which requires the presence of an additional 1-methylbenzimidazole, and remains as **2^{mbi}** in the cooled solution.

A similar analysis for the corresponding 1-methylimidazole complex, **2^{mi}-mi**, was not consistent with the presence of multiple species in solution (Figure 5, left). Although some of the peaks found at room temperature split and gave rise to new peaks as the solution was cooled down, the integration of the ^{1}H NMR spectrum at 213 K was consistent with the presence of only one compound (see the Supporting Information for integration data) that reflected the asymmetry of **2^{mi}-mi**. Cooling a toluene-d_8 solution of **2^{mi}** showed analogous results to those obtained in the case of **2^{mbi}**, indicating that the C_{2v}-symmetrical species was preserved (Figure 5, right). To summarize, neither of the 1-methylimidazole complexes, **2^{mi}** nor **2^{mi}-mi**, behaves like the coupled-mbi product, **3^{mbi}**, upon cooling.

^{2}H NMR spectroscopy experiments were also undertaken in order to gather additional information on the nature of the equilibria proposed in Scheme 3. In an effort to distinguish the different species present in solution (**2^{mbi}**, **2^{mbi}-mbi**, and/or **3^{mbi}**), the two- (**2^{mbi}-d_6**) and three-equivalent (**3^{mbi}-d_9**) 1-methylbenzimidazole products, as well as the two- (**2^{mi}-d_6**) and three-equivalent (**2^{mi}-mi-d_9**) 1-methylimidazole products, all deuterium-labeled at the methyl position, were studied by VT ^{2}H NMR spectroscopy. In the same fashion as the VT ^{1}H NMR study, **2^{mi}-d_6** and **2^{mi}-mi-d_9** (Figure 6, top left and right) as well as **2^{mbi}-d_6** (Figure 6, bottom left) showed no new peaks upon cooling. On the other hand, several new peaks were observed for the 1-methylbenzimidazole three-equivalent product, **3^{mbi}-d_9** (Figure 6, bottom right). The eight peaks observed in the −91 °C spectrum of **3^{mbi}-d_9** are consistent with the presence of two unsymmetrical species, which would each show three peaks, one symmetrical species (**2^{mbi}-d_6**, one peak, see Figure 6, bottom
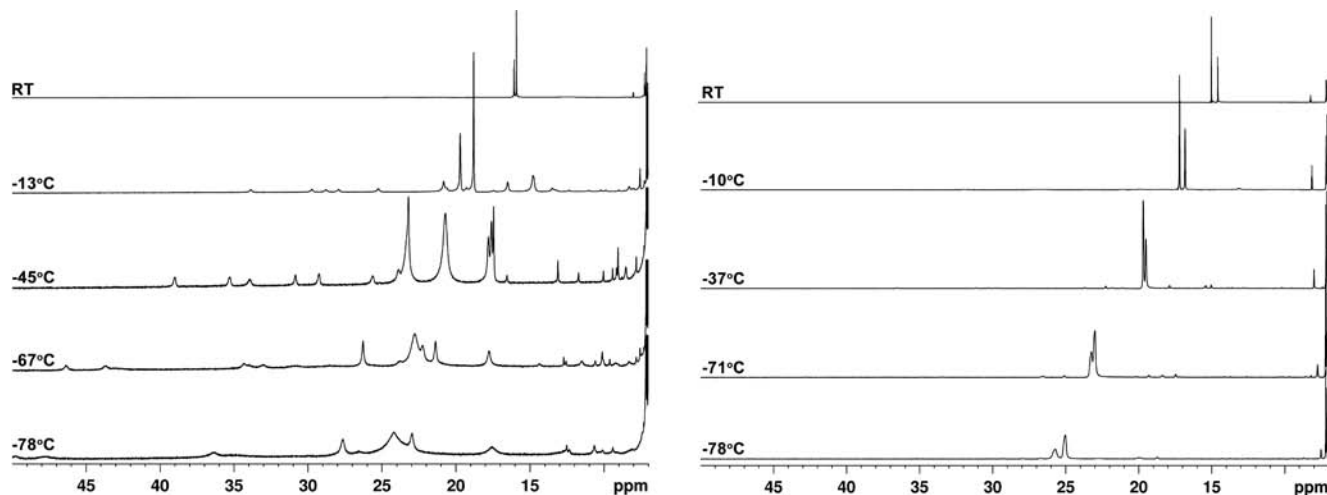
Figure 4. Variable-temperature ¹H NMR spectra of toluene-d_8 solutions of **3**[mbi] (*left*; note the appearance of several new peaks as the temperature is lowered) and **2**[mbi] (*right*; note that no new peaks become visible upon cooling), showing only one region at selected temperatures (see the Supporting Information for full spectra at all temperatures).
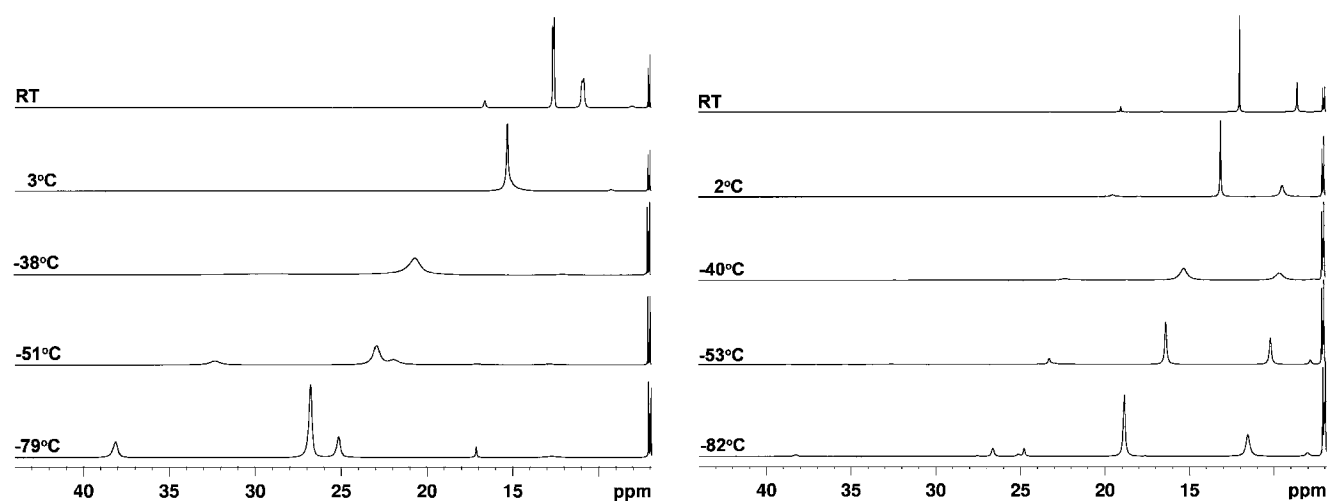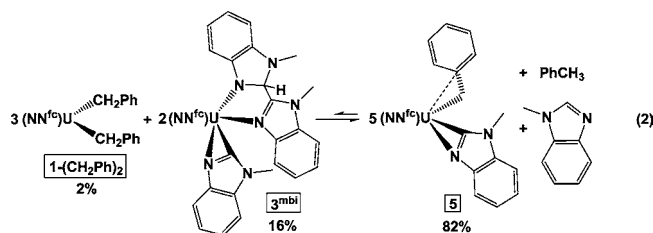

Figure 5. Variable-temperature ¹H NMR spectra of toluene-d_8 solutions of **2**[mi]**-mi** (*left*) and **2**[mi] (*right*), showing only one region at selected temperatures; note that both experiments are consistent with the presence of a single species in solution (see the Supporting Information for full spectra at all temperatures and integration data).

left), and free 1-methylbenzimidazole. The two unsymmetrical species could be **3**[mbi]**-d_9** and one of the isomers of **2**[mbi]**-mbi-d_9** or two isomers of **2**[mbi]**-mbi-d_9** (the cleavage of the C−C bond between the two coupled imidazole rings leading to these isomers could occur on the same time scale as the rotation of the coordinated 1-methylbenzimidazole ligand, as mentioned earlier).

The presence of these peaks is consistent with the equilibria depicted in Scheme 3 but, given the paramagnetic nature of the species involved, they do not offer additional information with respect to the identity of the species in solution. In principle, solid-state ¹³C NMR spectroscopy could answer the question whether compound **3**[mbi] exists only in the solid state or in solution as well. However, the solid-state ¹³C NMR spectrum acquired for a sample of **3**[mbi] showed only very broad peaks[47] that covered the entire region in which the solution spectrum showed peaks (see the Supporting Information).

Reactivity Studies. Reactivity studies offer direct support for the breaking of the C−C bond in **3**[mbi]. The reaction of **1-(CH₂Ph)₂** with **3**[mbi] in a 3:2 ratio afforded a new complex, **5** (eq 2). This reaction reached an equilibrium after 5 h, at which time **1-(CH₂Ph)₂**, **3**[mbi] (or a species related to it), and **5** were

present in 2, 16, and 82 mol %, respectively, as assessed by ¹H NMR spectroscopy. Although the chosen stoichiometry is consistent with the formation of one equivalent of free mbi, this was not detected by ¹H NMR spectroscopy, likely because it is engaged in a dynamic process with a species related to **3**[mbi] (represented as **3**[mbi] in eq 2 for simplicity). The direct synthesis of **5** from **1-(CH₂Ph)₂** and one equivalent of 1-methylbenzimidazole yielded dark-red crystals from a concentrated hexanes solution at −35 °C. X-ray crystallography revealed that **5** contains one benzyl and one η^2-N,C-imidazolyl ligand (Figure 7).

It is proposed that a comproportionation reaction takes place between **1-(CH₂Ph)₂** and either **2**[mbi] or **2**[mbi]**-mbi**, which are
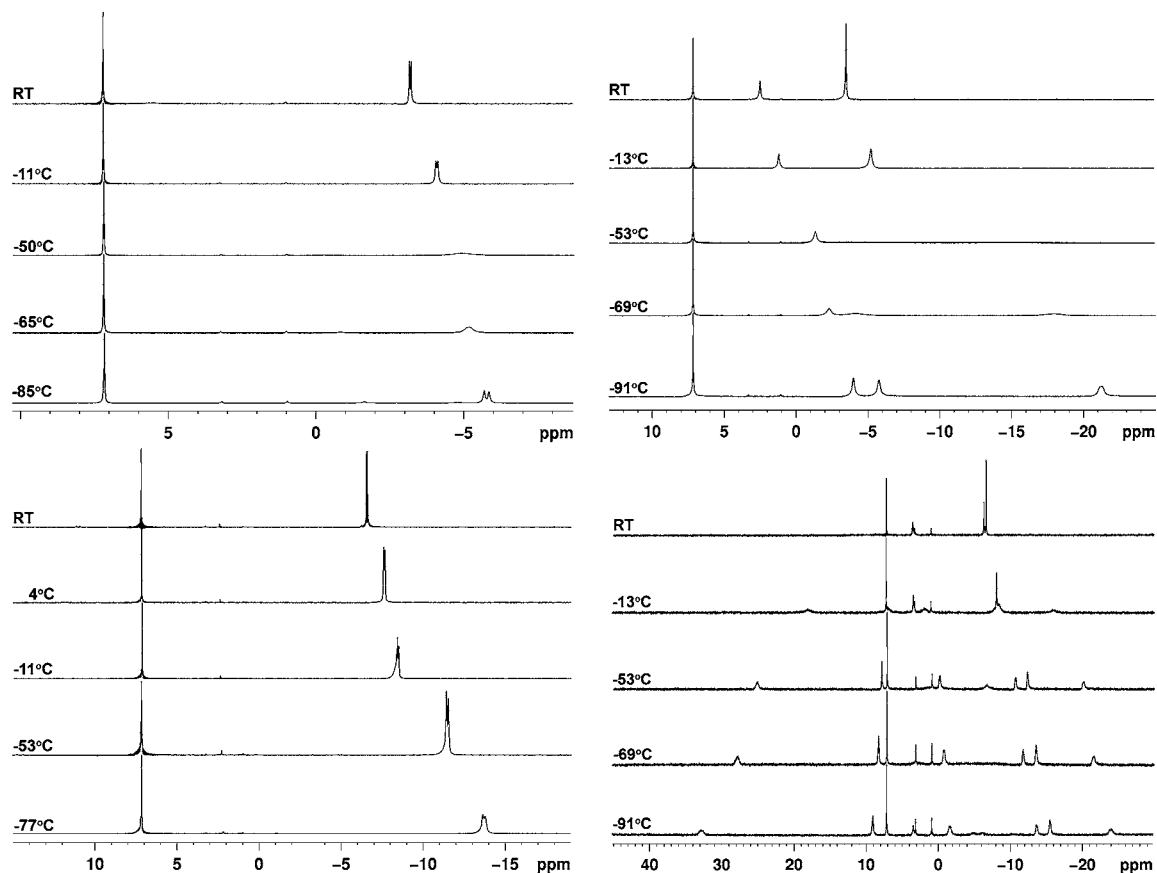
Figure 6. Variable-temperature ^{2}H NMR spectra of Et$_2$O solutions of **2^{mi}-d_6** (top left), **2^{mi}-mi-d_9** (top right), **2^{mbi}-d_6** (bottom left), and **3^{mbi}-d_9** (bottom right). Note that new peaks appear upon cooling only for **3^{mbi}-d_9**.
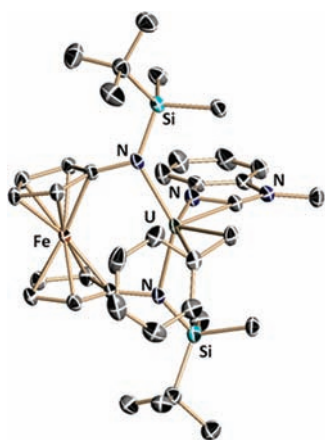

Figure 7. Thermal-ellipsoid (50% probability) representation of **5**; H atoms removed for clarity.

formed from **3^{mbi}** in solution (Scheme 3). An analogous reaction takes place between **1-(CH$_2$Ph)$_2$** and **2^{mi}-mi** (see the Supporting Information), lending further support to the reversibility of the C−C bond formation event in **3^{mbi}**.

In order to determine the sequence of events that led to the equilibrium shown in eq 2, the reaction of **1-(CH$_2$Ph)$_2$** with **3^{mbi}** in a 1:2 ratio was carried out (eq 3). The reaction mixture was then cooled to −72 °C and monitored by ^{1}H NMR spectroscopy. The resulting spectra matched those from the VT ^{1}H NMR experiment performed with **2^{mbi}** and not those from the analogous experiment carried out with **3^{mbi}**. These results show that **2^{mbi}** was cleanly produced in this reaction, as depicted in eq 3. Specifically, this experiment shows that (1) **3^{mbi}**

generated **2^{mbi}-mbi** in solution, (2) **2^{mbi}-mbi** lost its coordinated mbi, and (3) the free mbi then reacted and was C−H activated by both benzyl ligands of **1-(CH$_2$Ph)$_2$** to form **2^{mbi}**.

$$(3)$$
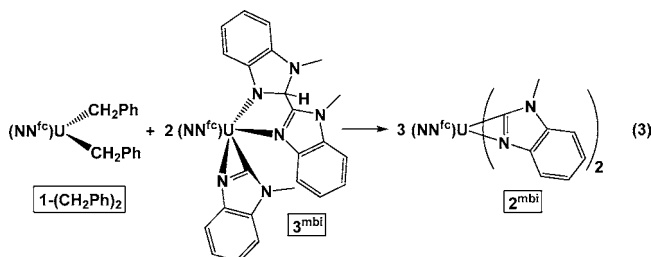
Finally, exactly one equivalent of **1-(CH$_2$Ph)$_2$** was added to the **2^{mbi}** produced in the above reaction. An equilibrium between the reactants and **5** was reached after one hour at room temperature (eq 4). This result shows that a comproportionation reaction occurs between **2^{mbi}** and **1-(CH$_2$Ph)$_2$**.
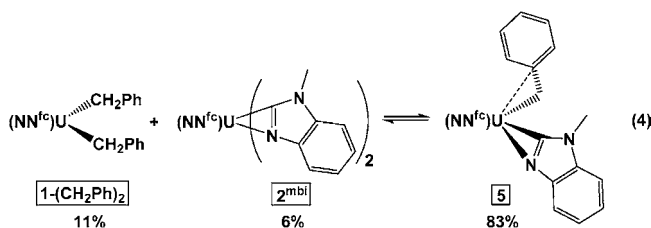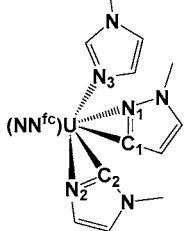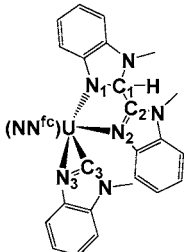

$$(4)$$

Table 1. Comparison of Metrical Parameters from Calculated (ADF) and X-ray Crystal Structures (Experimental Section) for 2^{mi}-**mi** and 3^{mbi}

Complex	Parameter	ADF	Experimental
2^{mi}-**mi**	U−N1	2.42 Å	2.42 Å
	U−N2	2.44 Å	2.41 Å
	U−N3	2.68 Å	2.61 Å
	U−C1	2.45 Å	2.47 Å
	U−C2	2.44 Å	2.47 Å
	N1−C1	1.35 Å	1.38 Å
	N2−C2	1.35 Å	1.36 Å
	U−N_{fc}	2.30 Å	2.28 Å
	U−N_{fc}	2.32 Å	2.32 Å
	N1UN2	119.0°	116.8°
	N2UN3	164.8°	166.9°
	N1UN3	76.0°	75.8°
	N_{fc}UN_{fc}	129.0°	131.0°
3^{mbi}	U−N1	2.38 Å	2.39 Å
	U−N2	2.59 Å	2.51 Å
	U−N3	2.41 Å	2.44 Å
	C1−C2	1.49 Å	1.49 Å
	U−C3	2.44 Å	2.46 Å
	N1−C1	1.45 Å	1.46 Å
	N2−C2	1.33 Å	1.33 Å
	N3−C3	1.36 Å	1.35 Å
	U−N_{fc}	2.24 Å	2.26 Å
	U−N_{fc}	2.27 Å	2.27 Å
	N1UN2	66.1°	66.2°
	N1UN3	151.3°	158.6°
	N2UN3	85.4°	93.5°
	N_{fc}UN_{fc}	125.6°	133.5°

DFT Calculations. DFT calculations were carried out with ADF2008.01[48−50] in order to understand why different complexes were isolated in the reactions between **1-(CH₂Ph)₂** and three equivalents of 1-methylimidazole versus 1-methylbenzimidazole. Calculations were performed on model compounds, in which the *tert*-butylsilyl substituents of the amide donors were replaced by methyl groups for economy. Geometry optimizations were carried out with relativistic corrections and the results indicated that the models showed similar metrical parameters to those obtained from the X-ray crystal structures for 2^{mi}-**mi** and 3^{mbi} (Table 1).

Once the validity of the calculations was established, calculations were carried out on models of the 1-methylimidazole analogue of 3^{mbi} and the 1-methylbenzimidazole analogue of 2^{mi}-**mi**. A comparison of the total bonding energies indicated that the two isomers of 2^{mi}-**mi-SiMe₃** considered were more stable than 3^{mi}-**SiMe₃** by 6.7 and 8.4 kcal/mol, while 3^{mbi}-**SiMe₃** was more stable than both isomers of 2^{mbi}-**mbi-SiMe₃** by 2.6 and 3.4 kcal/mol. The calculations therefore support our experimental observations: 2^{mi}-**mi** is more stable than 3^{mi} and 3^{mbi} is more stable than 2^{mbi}-**mbi**. The small energy difference between 3^{mbi}-**SiMe₃** and the isomers of 2^{mbi}-**mbi-SiMe₃** is also consistent with the fact that both forms of the compound may exist in solution.

The difference between the 1-methylimidazole and 1-methylbenzimidazole complexes can be visualized by inspecting the space-filling models of 2^{mi}-**mi** and 3^{mbi} (Figure 8); it is likely that the bulkiness of the three 1-methylbenzimidazole ligands determines that 3^{mbi} is more stable than 2^{mbi}-**mbi** because two
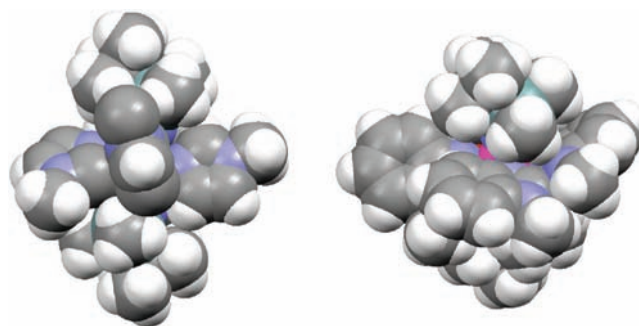
(47) Campbell, G. C.; Cotton, F. A.; Haw, J. F.; Schwotzer, W. *Organometallics* **1986**, *5*, 274.
(48) *ADF 2008 01; SCM;* http://www.scm.com: Theoretical Chemistry, Vrije Universiteit: Amsterdam, the Netherlands.
(49) Velde, G. t.; Bickelhaupt, F. M.; Baerends, E. J.; Fonseca Guerra, C.; van Gisbergen, S. J. A.; Snijders, J. G.; Ziegler, T. *J. Comput. Chem.* **2001**, *22*, 931.
(50) Fonseca Guerra, C.; Snijders, J. G.; te Velde, G.; Baerends, E. J. *Theor. Chem. Acc.* **1998**, *99*, 391.

Figure 8. Space-filling models of 2^{mi}-**mi** (left) and 3^{mbi} (right).

of the ligands may come into close contact by the formation of the C−C bond. The results of the DFT calculations and experimental studies presented above indicate that the C−C bond may be easily formed or broken in solution.

Conclusions

The product of the reaction between **1-(CH₂Ph)₂** and 1-methylbenzimidazole, 3^{mbi} was investigated: besides double C−H activation, a C−C coupling event took place in the uranium coordination sphere. Variable-temperature ¹H and ²H NMR spectroscopy studies support the proposal that the coupling is reversible in solution and isomers of 2^{mbi}-**mbi**, which do not contain a biheterocyclic fragment, are formed. Reactivity studies agreed with the existence in solution of 2^{mbi}-**mbi**. DFT calculations indicated that 3^{mbi} was indeed more stable than the analogue of 2^{mi}-**mi**, a situation reversed for 1-methylimidazole, but the energy difference between the two types of complexes is relatively small. Space-filling models for 2^{mi}-**mi** and 3^{mbi} helped to visualize that steric effects are likely responsible for the formation of the weak C−C bond between the two imidazole rings in 3^{mbi} in the solid state.

Experimental Section

All experiments were performed under a dry-nitrogen atmosphere using standard Schlenk techniques or an MBraun inert-gas glovebox. Solvents were purified using a two-column solid-state purification system by the method of Grubbs[51] and transferred to the glovebox without exposure to air. NMR solvents were obtained from Cambridge Isotope Laboratories, degassed, and stored over activated molecular sieves prior to use. Uranium turnings were purchased from Argonne National Laboratories. Compounds **1-(CH₂Ph)₂**,[33] 2^{mi}-**mi**,[21] 3^{mbi},[21] 1-methyl-d_3-imidazole,[52] and 1-methyl-d_3-benzimidazole[52] were prepared following published procedures. The aromatic heterocycles were distilled or recrystallized before use; all other materials were used as received. ¹H and ²H NMR spectra were recorded on Bruker300 or Bruker500 spectrometers at room temperature in C_6D_6 unless otherwise specified (Bruker300 and Bruker500 spectrometers are supported by the NSF Grant CHE-9974928). Chemical shifts are reported with respect to solvent residual peak, 7.16 ppm (C_6D_6). CHN analyses were performed by UC Berkeley Micro-Mass facility, 8 Lewis Hall, College of Chemistry, University of California, Berkeley, CA 94720.

Variable-Temperature (VT) NMR Experiments. Compounds were either isolated or synthesized in a J-Young NMR tube immediately prior to VT NMR experiments (see below). Samples were dissolved in diethyl ether for ²H NMR experiments (C_6D_6 was used as an internal reference) or toluene-d_8 for ¹H NMR experiments. Samples were cooled from room temperature to ca. −85 °C in increments of 5 or 10 °C. Post-experiment, room-temperature spectra were obtained to check for sample decomposition. Temperatures were calibrated with neat methanol.

2^{mi}: In a J-Young NMR tube, 1-methylimidazole (0.2 mL of a 0.34 M toluene-d_8 solution, 2 equiv) was added to **1-(CH$_2$Ph)$_2$** (0.0295 g dissolved in toluene-d_8) and placed in a 70 °C bath. After 45 min, the product had cleanly formed and no starting material remained, as determined by ^{1}H NMR spectroscopy.

2^{mi}-d_6: In a J-Young NMR tube, 1-methyl-d_3-imidazole (0.0051 g dissolved in diethyl ether, 2 equiv) was added to **1-(CH$_2$Ph)$_2$** (0.0248 g dissolved in diethyl ether). After one night at room temperature, the product had cleanly formed and no starting material remained, as determined by ^{1}H NMR spectroscopy.

2^{mbi}: To a diethyl ether solution of **1-(CH$_2$Ph)$_2$** (0.1863 g) was added a diethyl ether solution of 1-methylbenzimidazole (0.0570 g, 2 equiv). The reaction mixture was allowed to stir vigorously overnight at room temperature, then volatiles were removed under reduced pressure. The reaction was quantitative and the resulting dried product was used for VT NMR experiments with no further purification. *Note*: The dried solid is a film and could not be isolated in a crystalline or powder form; thus **2^{mbi}** could not be characterized by elemental analysis.

2^{mbi}-d_6: In a J-Young NMR tube, 1-methyl-d_3-benzimidazole (0.0078 g dissolved in diethyl ether, 2 equiv) was added to **1-(CH$_2$Ph)$_2$** (0.0250 g dissolved in diethyl ether). After one night at room temperature, the product had cleanly formed and no starting material remained, as determined by ^{1}H NMR spectroscopy.

2^{mi}-mi-d_9 and **3^{mbi}-d_9**: Syntheses were performed in the same manner as described previously for **2^{mi}-mi** and **3^{mbi}**,[21] using 1-methyl-d_3-imidazole and 1-methyl-d_3-benzimidazole. Isolated crystals were used in the VT NMR experiments.

Synthesis of 5. In a J-Young tube, **1-(CH$_2$Ph)$_2$** (0.0108 g in C$_6$D$_6$, 3 equiv) was added to **3^{mbi}** (0.0090 g in C$_6$D$_6$, 2 equiv). The reaction was monitored by ^{1}H NMR spectroscopy. After 5 h the reaction had ceased, and three compounds could be distinguished: **5** (82%), **3^{mbi}** (16%), and **1-(CH$_2$Ph)$_2$** (2%). In order to synthesize **5** directly, 1-methylbenzimidazole (0.0294 g, 1 equiv, in 2 mL toluene) was added to a stirring toluene solution (2 mL) of **1-(CH$_2$Ph)$_2$** (0.1920 g, 0.223 mmol). The mixture was allowed to stir until the ^{1}H NMR spectrum of an aliquot of the reaction showed that it was complete (8 h), at which time all three of the above-mentioned species were present in the same percentages. The volatiles were removed under reduced pressure, and the red-brown solids were dissolved in hexanes, filtered through Celite, concentrated, and placed in a −35 °C freezer. Crystals formed after several days. Yield: 0.0771 g, 38%. Anal. (%) for C$_{37}$H$_{52}$FeN$_4$Si$_2$U. Calcd: C, 49.22; H, 5.81; N, 6.21. Found: C, 49.52; H, 5.97; N, 6.13.

X-ray Crystal Structure of 5. The X-ray data collections were carried out on a Bruker AXS single crystal X-ray diffractometer using Mo Kα radiation and a SMART APEX CCD detector. The data was reduced by SAINTPLUS and an empirical absorption correction was applied using the package SADABS. The structures were solved and refined using SHELXTL (Bruker 1998, SMART, SAINT, XPREP, AND SHELXTL, Bruker AXS Inc., Madison, Wisconsin, U.S.A.).[53] All atoms were refined anisotropically, and hydrogen atoms were placed in calculated positions unless specified otherwise. Tables with atomic coordinates and equivalent isotropic displacement parameters, with all the bond lengths and angles, and with anisotropic displacement parameters, are listed in the text file for cif in Supporting Information.

X-ray quality crystals were obtained from a concentrated hexanes solution placed in a −35 °C freezer in the glovebox. Inside the glovebox, the crystals were coated with oil (STP Oil Treatment) on a microscope slide, which was brought outside the glovebox. A methylclopentane solvent molecule was found in the unit cell. The distance C1s−C5s was fixed to 1.54(1) Å. A total of 42868 reflections ($-22 \leq h \leq 22$, $-13 \leq k \leq 13$, $-40 \leq l \leq 39$) were collected at $T = 100(2)$ K with $\theta_{max} = 30.63°$, of which 12160 were unique ($R_{int} = 0.0369$). The residual peak and hole electron density were 1.05 and −0.82 e A^{-3}, respectively. The least-squares refinement converged normally with residuals of $R_1 = 0.0308$ and GOF = 1.020. Crystal and refinement data for **5**: formula C$_{43}$H$_{64}$N$_4$Si$_2$FeU, space group $P2_1/c$, $a = 16.538(3)$ Å, $b = 9.827(2)$ Å, $c = 27.945(6)$ Å, $\beta = 106.981(2)°$, $V = 4343.8(15)$ Å^3, $Z = 4$, $\mu = 4.146$ mm^{-1}, $F(000) = 1984$, $R_1 = 0.0440$ and $wR_2 = 0.0674$ (based on all 12610 data, $I > 2\sigma(I)$).

DFT Calculations. The Amsterdam Density Functional (ADF) package (version *ADF2008.01*)[48−50] was used to do geometry optimizations on Cartesian coordinates of the model compounds specified in the text. For the uranium and iron atoms, standard triple-ζ STA basis sets from the ADF database ZORA TZP were employed with 1s-2p (Si), 1s-3p (Fe), and 1s-5d (U) electrons treated as frozen cores. For all the other elements, standard double-ζ STA basis sets from the ADF database ZORA DZP were used, with the 1s electrons treated as a frozen core for non-hydrogen atoms. The local density approximation (LDA) by Becke−Perdew was used together with the exchange and correlation corrections that are employed by default by the ADF2008.01 program suite. Calculations for all model compounds were carried out using the spin-unrestricted, scalar spin−orbit relativistic formalism.

Supporting Information Available: Details for the NMR spectroscopy experiments, DFT calculations, and full crystallographic descriptions (cif as text). This material is available free of charge via the Internet at http://pubs.acs.org.

JA9109715

(51) Pangborn, A. B.; Giardello, M. A.; Grubbs, R. H.; Rosen, R. K.; Timmers, F. J. *Organometallics* **1996**, *15*, 1518.
(52) Pilarski, B. *Liebigs Ann. Chem.* **1983**, *1983*, 1078.
(53) Sheldrick, G. *Acta Crystallogr., Sect. A* **2008**, *64*, 112.